

# Photo-Induced Relaxation and Proton Transfer in Some Hydroxy Naphthoic Acids in Polymers

Hirdyesh Mishra\*

Photophysics Laboratory, Department of Physics, Kumaun University, Nainital-263 001, India

Received: May 7, 2005; In Final Form: March 9, 2006

Photophysical and photochemical properties of 3-hydroxy-2-naphthoic acid [3,2-HNA] and 1-hydroxy-2-naphthoic acid [1,2-HNA] in different aprotic, protic, and ion exchange (Nafion) polymers have been described in this article. In both molecules, intramolecular hydrogen bond (IMHB) exists between OH and COOH functional groups. Both 3,2-HNA and 1,2-HNA form different emitting species in different polymeric media. Fluorescence characteristic of 3,2-HNA is found to depend on its concentration, nature of the microenvironment, and wavelength of excitation, while 1,2-HNA is less susceptible to these changes. 3,2-HNA exhibits dual fluorescence band (normal and large Stokes shifted) in aprotic and only a single large Stokes shifted fluorescence in protic polymers, while 1,2-HNA shows a single fluorescence band along with weak phosphorescence emission in these polymers. Both excited-state inter and intramolecular proton transfer (ESPT) take place in 3,2-HNA in aprotic and protic polymers, resulting in large Stokes shifted emission band. A competition between ESIPT and excimer formation is observed by the appearance of rise time on increasing the concentration of 3,2-HNA in protic polymer. In Nafion film, 3,2-HNA is present as a cationic as well as neutral species. The presence of extra protons in Nafion film facilitates excited-state intramolecular proton transfer (ESIPT) in the neutral species of 3,2-HNA and gives large Stokes shifted emission ( $10\,500\text{ cm}^{-1}$ ). No such effect is observed in 1,2-HNA doped in Nafion film. It is observed that, depending on the position of the IMHB ring, the electronic spectra get modified and the strength of IMHB is affected by the micro-environment of the polymer which alters the photophysics of these molecules.

## 1. Introduction

The photoinduced excited-state relaxation processes in various polymers are useful for studying different specific interactions between dye and host polymers, and they have been found to change the photophysics and photochemistry of excited molecules in the presence of various polymer micro environmental effects.<sup>1–3</sup> In fluid media, the fluorescence occurs at the same wavelength irrespective of the excitation frequency because of the fast relaxation time ( $\tau_r$ ) in comparison with the excited-state lifetime ( $\tau_f$ ), and a dynamic equilibrium exists among these solvation sites. In rigid media, however, the dynamic equilibrium among different solvation sites is lost and emission occurs from the Frank Condon (FC) State that corresponds to the solvation site specifically excited, because the relaxation rate constant of different solvation sites is different. This leads to an excitation wavelength dependence of fluorescence parameters.<sup>4</sup> Additionally, in rigid medium, nonradiative losses due to rotational restrictions and diffusion quenching are decreased.<sup>5</sup> Birch et al.<sup>6</sup> found that the kinetics of the fluorophores are more complicated in polymers because of the presence of distribution of decay times.

Studies of excited-state inter/intramolecular proton transfers (ESPT) in hydrogen bonded systems are of great interest for investigating the structure and dynamics of polymers. Recently, dyes showing ESPT have been demonstrated in some intramolecular hydrogen bonded (IMHB) polymers of interest as triplet quencher,<sup>7</sup> photochromic materials,<sup>8</sup> polymer lasers,<sup>9–10</sup> optical sensors,<sup>11–13</sup> luminescence solar collectors,<sup>14</sup> optical switches,

memory devices, photostabilizers,<sup>15</sup> etc. Effect of different micro-heterogeneous environment on excited-state proton-transfer characteristics with different molecules in membrane mimetic system appears in the literature.<sup>16–20</sup>

In our earlier work, we had reported the photophysics of 3-hydroxy 2-naphthoic acid (3,2-HNA) and 1-hydroxy 2-naphthoic acid (1,2-HNA), in detail, in fluid and in crystalline state<sup>21–24</sup> using experimental and theoretical computational calculations. These molecules were formed by substitution of  $-\text{OH}$  and  $-\text{COOH}$  group in the naphthalene ring at  $\beta-\beta$  position (3,2-HNA) and  $\alpha-\beta$  position (1,2-HNA), respectively. IMHB is formed between OH and COOH functional groups and stability of IMHB in these molecules has been reported by Golubev et al.<sup>25</sup> Hydroxy naphthoic acids are of interest for understanding the effect of IMHB in the photostability and in excited-state intramolecular proton transfer (ESIPT). These molecules are used as chelating agents, fluorescent indicators, and the manufacture of dyestuffs.<sup>26</sup> We have also found that the chelates formation is easy in 3,2-HNA, in comparison to 1,2-HNA or 2,1-HNA. In 3,2-HNA, ESIPT is observed in neutral as well as in monoanionic form, while in case of 1,2-HNA, ESIPT is observed only in monoanionic species. Besides this, the keto form of monoanionic species of 1,2-HNA is more stable in ground state and, hence, ground-state intramolecular proton transfer (GSIPT) is also observed in it.<sup>24</sup> The difference between the photoinduced excited-state relaxation processes has been attributed to the change in the geometry and acid–base properties of these molecules. The computational calculations reveal that the strength of intramolecular hydrogen bonds is higher in monoanion of 1,2-HNA as compared to that of 3,2-

\* Corresponding author. Fax: +91-5942-235576. E-mail: hirdyesh@yahoo.com.

HNA.<sup>23</sup> The  $L_a$  and  $L_b$  bands appear to play an important role in understanding the photophysics of these molecules. Here the  $L_a$  and  $L_b$  refer to polarization of the excited state along the axis through the atoms and the axis through the bonds, respectively.<sup>27</sup> It is also known that the lowest energy transition in case of molecules having cross-linking with the conjugated chain is  $L_b$ .

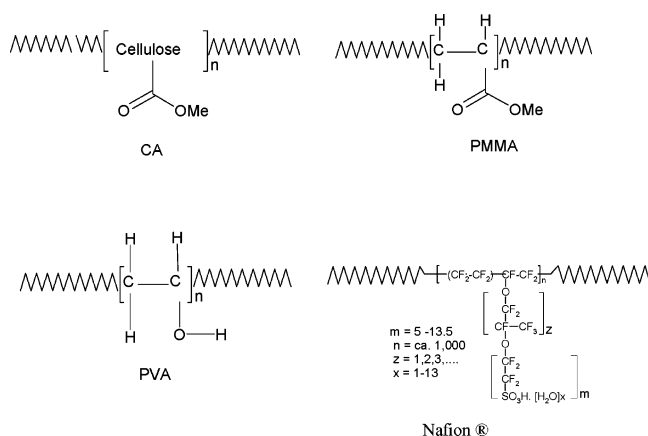
Earlier the photophysics of methyl 3-hydroxy-2-naphthoate and phenyl 1-hydroxy-2-naphthoate was investigated by Woolfe and Thistlethwaite.<sup>28,29</sup> They found that the former gave rise to large Stokes shifted emission, while the latter exhibited only normal emission. This difference has been attributed to the difference in the acid–base properties of the two species. Law and Shoham<sup>30</sup> also reported the photophysics of methyl 3-hydroxy-2-naphthoate (3,2-MHN) in nonpolar and polar solvents and found ESIPT to be solvent and temperature dependent. Kovi and Schulman<sup>31,32</sup> have identified several species of hydrogen bonded hydroxy naphthoic acids under different pH conditions. Substitution of a phenyl ring in  $\alpha$ -position in naphthoic acid causes level inversion, while in  $\beta$  position no such level inversion takes place.<sup>33</sup> Catalán et al.<sup>34</sup> have shown that photostability of methylated derivative of these compounds are independent of the photophysics of their proton-transfer tautomers but depends on the nonradiative dynamics of their respective normal tautomers. Banerjee et al.<sup>35</sup> have studied 3,7-dihydroxy-2-naphthoic acid in protic and aprotic solvents and found evidence for the existence of both the monomer and the dimer in very dilute solutions. They also proposed that addition of a base promotes proton transfer in polar protic solvents only. Recently, effect of different micelles environment on the ESIPT in 2-hydroxy-3-naphthaldehyde (HNL) has been studied by Chowdhury and Chakravorti.<sup>36</sup> They found that deprotonation of HNL is retarded in neutral and anionic micelles than in cationic micelles. In neutral micelles nonradiative process is less affected as compared to ionic micelles.

In the present work, we have studied the photophysics and photochemistry of 3,2-HNA and 1,2-HNA in different aprotic viz. polymethyl methacrylate (PMMA), cellulose acetate (CA), protic viz. poly(vinyl alcohol) (PVA), and Nafion (ion exchange and hydrophilic) polymer matrixes. We have reported how the polymeric microenvironment affects the excited-state proton switching and triplet emission in these molecular systems under different concentrations and wavelength of excitation. The changes in fluorescence intensity and decay in these molecules taken in different polymers are correlated with free volume and micro-polarity of the polymers. A brief comparison of the photophysics of 3,2-HNA with 1,2 HNA is also discussed.

## 2. Experimental Section

**2.1. Materials.** 3,2-HNA and 1,2-HNA, (Aldrich chemical company Inc., U.S.A), were purified by an ethanol–water mixture and re-crystallized from ethanol. Aprotic polymers viz. polymethyl methacrylate PMMA (L) having low density (M. W. 12 000) and PMMA (H) high density (M. W. 96 000) and Cellulose acetate (CA) (average molecular weight 30 000), protic polymer polyvinyl alcohol PVA (average molecular weight: 1700–1800), were purchased from Aldrich and used as such. Nafion 117 film from Aldrich (average M. W. 1100) is cleaned by boiling with nitric acid for about 45 min to remove the impurities and then boiled with water for about 90 min and then washed by HPLC water. The cleanliness of the film is checked by UV–visible absorption spectrum. All the solvents were either of spectroscopic grades or were checked for their fluorescence purity. The molecular structural formulas of these four polymers are shown in Scheme 1.

## SCHEME 1: Molecular Structural Formulas of Different Polymers



**2.2. Preparation of the Film.** 3,2-HNA and 1,2-HNA (probe molecules) doped CA films were prepared by dissolving the required quantity of the probe fluorophore powder in acetone and mixing it with the desired concentration of probe molecules in a solution of acetone. The resultant mass was spread in a polypropylene dish to obtain a film. Probe molecules doped in PMMA films were prepared by dissolving PMMA grains in dichloromethane (DCM) and mixing it with the desired concentration of probe molecules in DCM. The films were again obtained by drying the mass in a polypropylene dish. Probe molecules doped PVA films were prepared by mixing PVA grains with desired amount of it and dissolving it in hot water (40 °C). The mass was spread in a polypropylene dish and was dried in an incubator. The estimated concentration of different films is about 0.05 and 0.5 wt % weight percentile. Probe molecules having concentration of  $10^{-4}$  M in water were incorporated separately into Nafion film. The dye loaded film was dipped in clean water to ensure the release of the unbound dye molecules. The spectrum of the loaded film did not change even after several weeks in the lab. The concentration of the dye in the Nafion film was estimated optically by absorption spectra of the loaded film and taking into consideration the extinction coefficient of the dye. It was nearly about  $10^{-5}$  M. Purity of the reference films was checked by fluorescence run test of the neat polymer film.

**2.3. Instrumentation.** Absorption and corrected emission/excitation spectra were recorded by using JASCO V-550 spectrophotometer and JASCO FP-777 spectrofluorometer, respectively.<sup>37</sup> Sample films of dimension approximately 30 mm  $\times$  10 mm  $\times$  0.2 mm was held in 1 cm quartz cuvette in right angle geometry. Fluorescence decay times were recorded with the help of Edinburgh FLA-199 spectrometer. The excitation source was a thyatron gated hydrogen filled nanosecond flash lamp. Lamp profile was measured at the excitation wavelength using Ludox scatterer. The pulse width was about 1.0 ns with repetition rate of 20 kHz. Time correlated single photon counting (TCSPC) technique was used to collect the decay curves and the resolution of the system is about 200 pico-second. Intensity decay curves so obtained were fitted to sum of exponential terms as shown:

$$I(\tau, t) = \sum_i \alpha_i e^{-t/\tau_i}$$

where  $\tau_i$  are the multiple fluorescence decay times and  $\alpha_i$  are the corresponding amplitudes. Appearance of negative amplitude indicates the rise time due to some excited state processes. Weighted residuals and  $\chi^2$  values are used to judge the goodness

**TABLE 1: Photophysical Parameters of 3,2-HNA in Different Polymers**

polymer	$\lambda_{ab}$ (nm)	$\lambda_{em}$ (nm)	stokes shift $\sim\{\nu_{exc} - \nu_{em}\}$ ( $cm^{-1}$ )	mean decay time $\langle\tau\rangle$ (ns)	hydrogen bonded emitting species
PMMA (L)	364	420	3600 (B)	13.6	rotamer P,
		515	7900 (G)	0.89	rotamer R
				4.54	monoanion
PMMA (H)	366	420	3500 (B)	14.2	rotamer P,
		515	7900 (G)	0.81	rotamer R
				4.59	monoanion
CA	363	420	3700 (B)	15.9	rotamer P,
		515	7940 (G)	0.83	rotamer R
				5.73	monoanion
PVA	352	510	8800 (G)	10.9	rotamer P,
		480 (hump)	4200 (B)	1.35	rotamer R
				4.65	monoanion
Nafion	376	420	3900 (B)	10.2	rotamer P
	425	530	4600 (G)	0.49	rotamer P
		580	10500 (R)	2.8	monocation
				0.39	tautomer R

of fits. The average decay time for triple-exponential decay of fluorescence was calculated from the observed decay times and preexponential factors using the following equation:<sup>2</sup>

$$\langle\tau\rangle = \frac{\sum_{i=1}^3 \alpha_i \tau_i^2}{\sum_{i=1}^3 \alpha_i \tau_i}$$

### 3. Results and Discussion

**3.1. 3-Hydroxy-2-Naphthoic Acid (3,2-HNA).** The steady state and time domain parameters of 3,2-HNA in different polymers are given in Table 1 to 4, respectively.

**3.1.1. In Aprotic Polymers.** In aprotic polymers viz. PMMA and CA (hydrogen bonding in nature), 3,2-HNA shows two absorption bands at 280 nm ( $L_a$ ) and 366 nm ( $L_b$ ), respectively. The absorption spectra of 3,2-HNA in low molecular weight PMMA (L), at 0.05 wt % and 0.5 wt % concentration are shown in Figure 1a. The corresponding dual emission at 420.0 nm (blue B band) and 515.0 nm (green G band) are observed in these polymers. The Gaussian peak fit analysis of emission spectra of 3,2-HNA in PMMA shows three peaks at 410, 450, and 525 nm, respectively, as shown in Figure 1b.

The intensity ratio of B and G bands depends strongly on the wavelength of excitation as shown in Figure 2a and b for PMMA (L) and CA, respectively. With shorter wavelengths, excitation, intensity of G band increases, while on excitation with longer wavelengths, the intensity of B band increases. The excitation spectrum corresponding to B band is structured, whereas for G band, it shows broad band and blue shifted as shown in Figure 2c and d for PMMA (L) and CA, respectively. The Stokes shifts of B and G bands corresponding to their excitation frequencies are  $\sim 3600\text{ cm}^{-1}$  and  $\sim 7900\text{ cm}^{-1}$ , respectively, as given in Table 1. On increasing the concentration (0.5 wt %), the absorption spectrum becomes more structured while emission spectrum shows decrease in relative intensity of G band. These observations rule out the possibility of dimer formation. The Intensity of G band increases in the order of PMMA (L) < PMMA (H) < CA in these aprotic polymers.

Further during polymerization of the film, a weak emission at 580 nm (red band) is also observed besides the blue emission. This red band disappears in the final rigid state of the film. Similar results were observed in the temperature variation in 3,2-HNA in acidic ethanol<sup>21</sup> and were explained on the basis of the presence of neutral species, in which ESIPT takes place in liquid form of the polymer film. Thus this red band (580 nm) is due to ESIPT in neutral species in solution phase. On

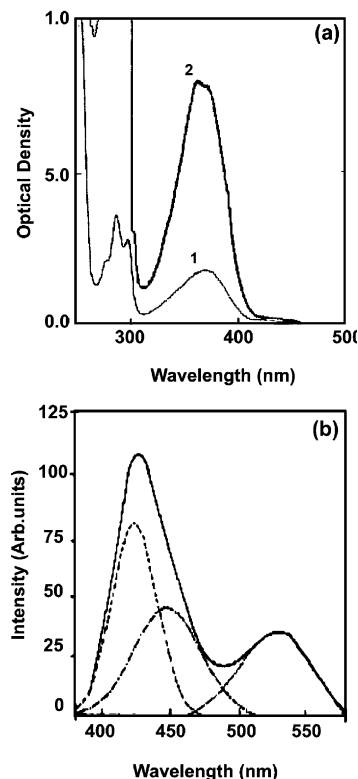


**Figure 1.** (a) Absorption spectra of 3,2-HNA in PMMA (L) at (1) 0.05 wt % and (2) 0.5 wt % concentration. (b) Gaussian peak fit analysis of the emission band of 3,2-HNA in PMMA polymer.

increasing rigidity, disappearance of the red band and appearance of green emission (G band) indicates that the neutral species are converted into hydrogen bonded species due to an increase of the interaction of dye to host polymer in which ground-state intermolecular proton transfer from dye to polymeric media takes place. Simultaneously, ESIPT takes place in this hydrogen-bonded monoanion due to formation of strong intramolecular hydrogen bond. Disappearance of ESIPT band (580 nm) in remaining neutral species (P) on increasing the rigidity may be due to the change in the favorable geometry. Similar changes in the electronic transitions were observed by Fuji et al.<sup>38</sup> in methyl salicylate doped in sol-gel and gel-xerogel mixture solution during the transition period of stabilization.

The decay curve of 3,2-HNA in polymers PMMA (L) and CA at different emission wavelengths are shown in Figure 2e and f. In these aprotic polymers, 420 nm fluorescence decay fits to a triple exponential function with decay times as 13.0, 4.5, and 0.90 ns, respectively, as shown in Table 2. The amplitudes of 13.0 ns and 4.5 ns decay components decrease, while amplitude of shorter decay component 0.90 ns increases toward a longer wavelength of the emission spectrum. The increase in decay time of these species in these polymers as compared to the fluid solution indicates that the rigidity of the matrix decreases the nonradiative transition as in case of salicylic acid (SA).<sup>22,39</sup> Like SA, in 3,2-HNA emission from both rotamer R (absence of intramolecular hydrogen bond) and rotamer P (presence of intramolecular hydrogen bond) along with monoanion is observed in aprotic polymers. On comparing the two, it is found that, in the above three polymers, the intensity and magnitude of decay times decrease in the order of CA > PMMA (H) > PMMA (L). This behavior of fluorescence parameters may be due to change in free volume for different polymers. It is known that availability of greater free volume will increase the nonradiative processes which will reduce the magnitude of

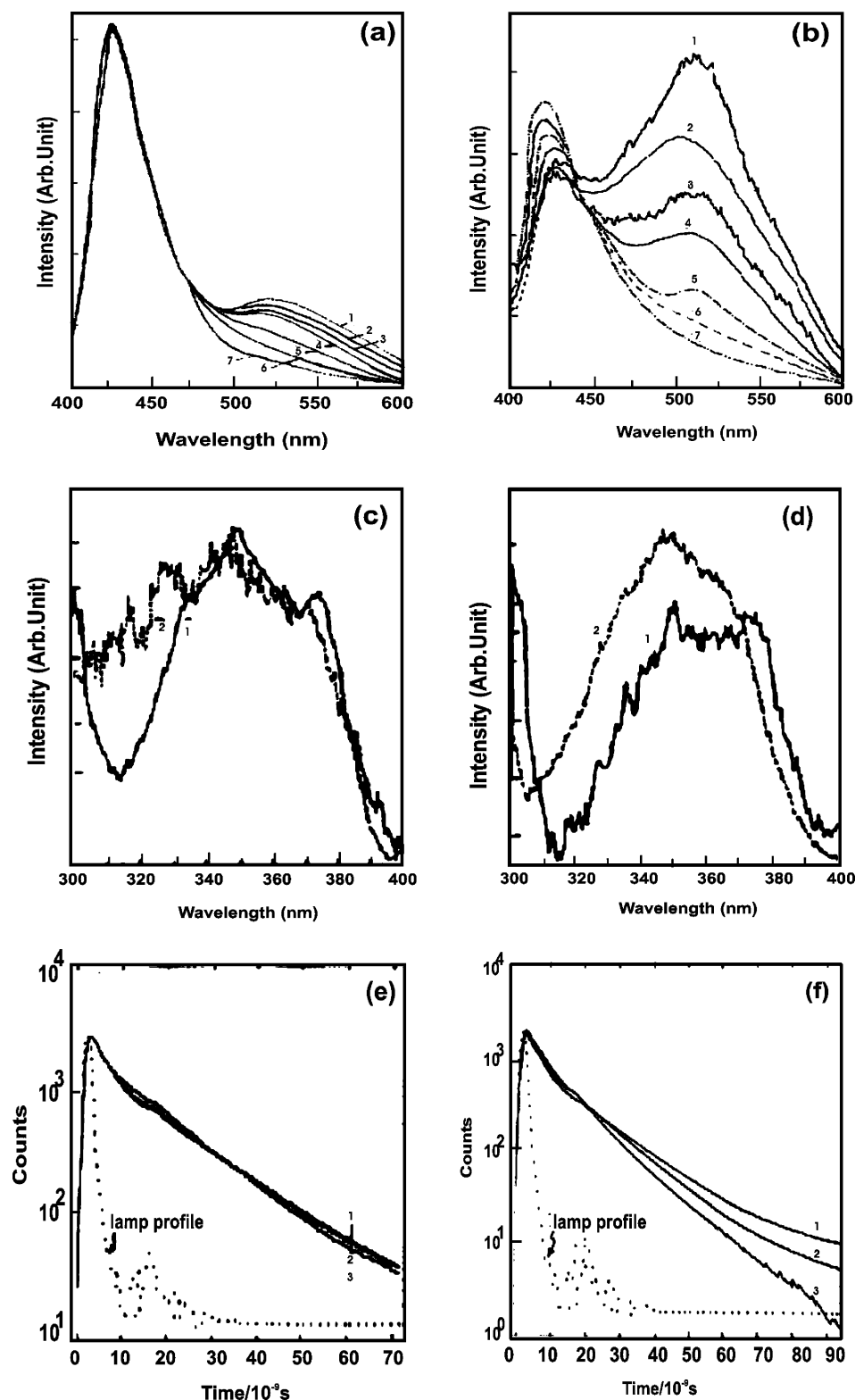


**Figure 2.** Normalized overlapped emission spectra of 3,2-HNA in (a) PMMA (L) and (b) CA [ $\lambda_{ex}$  = (1) 300 nm, (2) 310 nm (3) 320 nm, (4) 330 nm, (5) 340 nm, (6) 360 nm, (7) 370 nm.]. Normalized overlapped excitation spectra of 3,2-HNA in (c) PMMA (L) and (d) CA [ $\lambda_{em}$  = (1) 450 nm, (2) 510 nm]. Overlapped decay curves of 3,2-HNA in (e) PMMA (L) and (f) CA, [ $\lambda_{ex}$  = 330 nm and  $\lambda_{em}$  = (1) 420 nm, (2) 460 nm, (3) 530 nm] at 0.05 % wt concentration.

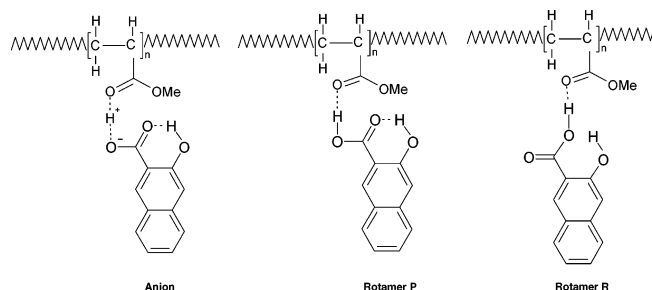
the fluorescence intensity and decay time. The origin of above emissions may result from three different hydrogen bonded emitting species viz, rotamers R and P and their hydrogen-bonded monoanions in analogy with the solution phase spectra.<sup>21</sup> The presence of various emitting species in these polymers are shown in Scheme 2.

Hydrogen bonded rotamer P and R species of 3,2 HNA give overlapped normal blue emission, while large Stokes shifted green emission is observed in hydrogen-bonded monoanionic species, which is formed due to intermolecular proton transfer from carboxylic proton of 3,2-HNA in rotamer P to proton acceptor site of the host polymer chain. Upon increasing the



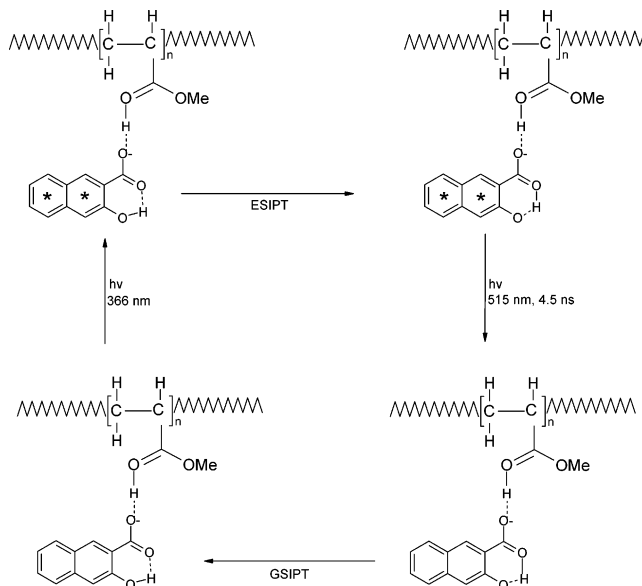
**TABLE 2: Decay Data of 3,2-HNA in Aprotic Polymers:  $\lambda_{\text{Ex}} = 350$  nm**

P	(M)	Em	$\tau_{1(\text{ns})}$	$\tau_{2(\text{ns})}$	$\tau_{3(\text{ns})}$	$\alpha_1\%$	$\alpha_2\%$	$\alpha_3\%$	$\chi^2_3$	$\chi^2_2$
PMMA (L)	0.02 wt. %	420	$13.7 \pm 0.02$	$0.87 \pm 0.09$	$4.48 \pm 0.02$	52	11	37	1.135	1.567
	0.02 wt. %	460	$13.9 \pm 0.03$	$0.94 \pm 0.07$	$4.40 \pm 0.01$	50	15	35	1.064	1.436
	0.02 wt. %	500	$13.4 \pm 0.02$	$0.86 \pm 0.04$	$4.75 \pm 0.02$	49	18	33	1.010	1.759
	0.5 wt. %	420	$13.5 \pm 0.03$	$1.01 \pm 0.01$	$4.19 \pm 0.30$	55	12	33	1.190	1.349
	0.5 wt. %	460	$13.9 \pm 0.09$	$1.40 \pm 0.02$	$4.75 \pm 0.08$	44	26	30	1.165	1.359
	0.5 wt. %	500	$13.4 \pm 0.03$	$0.98 \pm 0.05$	$4.11 \pm 0.10$	42	30	28	1.021	1.287
PMMA (H)	0.02 wt. %	420	$14.2 \pm 0.01$	$0.79 \pm 0.09$	$4.50 \pm 0.03$	53	14	33	1.009	1.489
	0.02 wt. %	460	$14.8 \pm 0.07$	$0.77 \pm 0.07$	$4.62 \pm 0.02$	50	18	32	1.102	1.407
	0.02 wt. %	500	$13.8 \pm 0.10$	$0.89 \pm 0.05$	$4.66 \pm 0.02$	48	24	28	1.110	1.352
	0.5 wt. %	420	$15.0 \pm 0.05$	$0.99 \pm 0.01$	$4.89 \pm 0.03$	60	7	33	1.139	1.501
	0.5 wt. %	460	$13.4 \pm 0.03$	$0.84 \pm 0.05$	$4.29 \pm 0.03$	56	14	30	1.111	1.486
	0.5 wt. %	500	$12.8 \pm 0.03$	$0.64 \pm 0.09$	$4.58 \pm 0.04$	47	28	25	1.029	1.389
CA	0.02 wt. %	420	$16.5 \pm 0.05$	$0.70 \pm 0.01$	$5.60 \pm 0.02$	56	6	38	1.063	1.277
	0.02 wt. %	460	$15.3 \pm 0.09$	$0.96 \pm 0.01$	$5.90 \pm 0.05$	53	12	35	1.028	1.254
	0.02 wt. %	500	$15.9 \pm 0.04$	$0.85 \pm 0.07$	$5.70 \pm 0.01$	50	20	30	1.069	1.373
	0.5 wt. %	420	$16.2 \pm 0.04$	$0.99 \pm 0.01$	$4.10 \pm 0.03$	60	8	32	1.078	1.246
	0.5 wt. %	460	$16.2 \pm 0.01$	$1.03 \pm 0.01$	$4.75 \pm 0.08$	53	17	30	1.113	1.645
	0.5 wt. %	500	$16.1 \pm 0.03$	$0.98 \pm 0.02$	$4.91 \pm 0.04$	50	22	28	1.069	1.137

**SCHEME 2: Presence of Various Emitting Species of 3,2-HNA in Aprotic Polymers**

concentration of 3,2-HNA, intensity of G band decreases, which may be due to decrease of dissociation of 3,2-HNA (common ion effect). A comparison of the decay times of 3,2-HNA in polymer hosts with those obtained in solution phase (in hydrogen bonding aprotic solvents<sup>21</sup>). It is found that the decay time of 13.0 ns corresponds to hydrogen bonded rotamer R, shorter decay time 0.9 ns corresponds to hydrogen bonded rotamer P and the decay time 4.5 ns corresponds to monoanion of hydrogen-bonded species of 3,2-HNA showing excited-state intramolecular proton transfer (ESIPT) as shown in Scheme 3.

**3.1.2. In Protic Polymer.** In PVA, which is polar and hydrogen bonded in nature, 3,2-HNA (0.02 wt %) shows absorption maximum at 352 nm and emission bands at 510 nm (G band) with a hump at 420 nm (B band) as shown in Figure 3a and b, respectively. The Stokes shifts of these emission bands are  $\sim 8800$   $\text{cm}^{-1}$  and  $\sim 4200$   $\text{cm}^{-1}$ , respectively, as given in Table 1. The absorption of 3,2-HNA in PVA is about  $\sim 12$  nm blue shifted (352 nm) as compared to that in aprotic polymer PMMA. The excitation spectra monitored at the blue edge and red edge of the emission is structured and broad banded respectively as shown in Figure 3c. At higher concentrations (0.5 wt %), the G emission band shows a red shift with decrease in full width half-maximum (fwhm) as shown in Figure 3d. The excitation spectra are structured for both B and G emission bands at higher concentration. Similar to aprotic polymers, this shows presence of three emitting species viz. hydrogen bonded rotamer R, P and monoanion. The decrease in intensity of blue emission shows the percentage of rotamer R is lower in this polymer. Further, it is observed that the percentage of rotamer P increases and monoanion decreases with increase of concentration. With addition of  $\text{H}^+$  ion (using  $\text{H}_2\text{SO}_4$ ) in this matrix only B emission is observed, which is independent of wavelength of excitation and its excitation spectrum is structured. This emission corre-

**SCHEME 3: Excited State Intra Molecular Proton Transfer (ESIPT) in Mono-anion of 3,2-HNA**

sponds to neutral species. However, on addition of  $\text{OH}^-$  ion (using alkali) in this matrix, only G band is observed, having broadband excitation spectrum. This indicates that upon adding alkali only monoanion is formed, which undergoes ESIPT. Unlike aprotic polymers, no red emission (red band) is observed in the solution phase of the PVA polymer. This indicates the interaction of dye to host polymer is strong, even in solution phase of the protic polymer with respect to aprotic polymer.

The time domain measurements (Table 3), shows that the emission decay fits to a triple exponential function throughout the emission profile with average decay times 11.0, 4.5, and 1.4 ns, respectively. On monitoring the emission decay toward the red edge of the emission profile, the amplitude of 4.5 ns decay time increases, while amplitudes of 11.0 ns and 1.4 ns decrease, as shown in Figure 3d. In analogy with solution phase (in hydrogen bonding protic solvents kinetic data<sup>21</sup>), it is found that a longer decay time 11.0 ns corresponds to hydrogen bonded rotamer R, shorter decay time of 1.4 ns corresponds to hydrogen bonded rotamer P, and the decay time of 4.5 ns corresponds to anion of rotamer P, which shows excited-state intramolecular proton transfer. Unlike aprotic polymers, upon increasing the concentration, the intensity of blue emission decreases (Figure 3e) and a rise time is observed in green emission as shown in

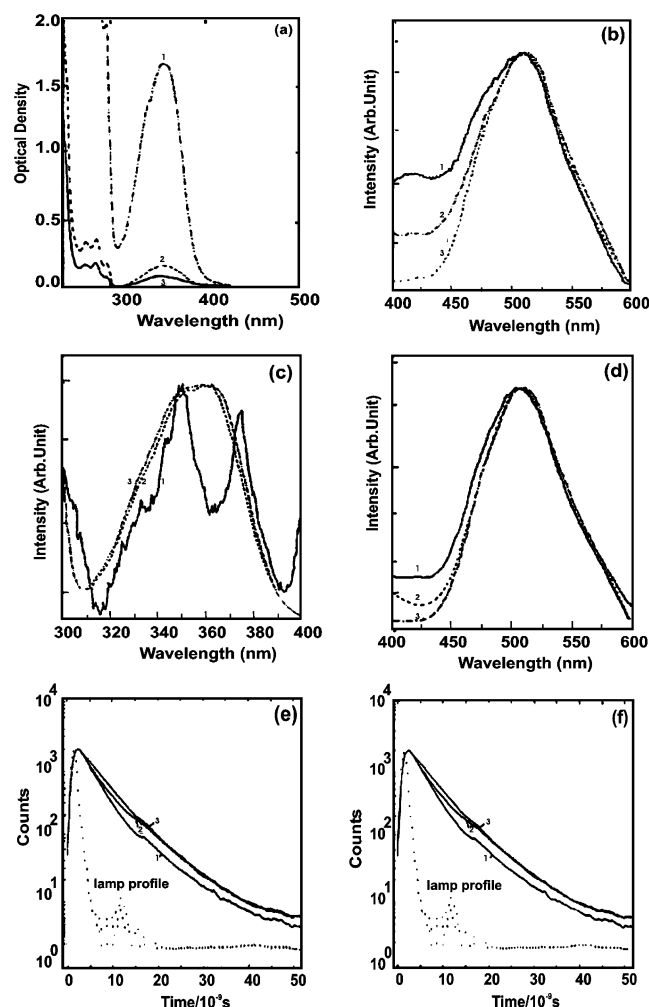


**Figure 3.** (a) Overlapped Absorption spectra of 3,2-HNA in PVA at concentration (1) 0.5 wt %, (2) 0.05 wt %, (3) 0.02 wt %. Normalized overlapped emission spectra of 3,2-HNA in PVA at concentration (b) 0.05 wt % and (d) 0.05 wt %, [ $\lambda_{\text{ex}}$  = (1) 310 nm, (2) 350 nm, (3) 375 nm]. Normalized excitation spectra of 3,2 HNA in PVA at concentration (c) 0.05 wt % [ $\lambda_{\text{em}}$  = (1) 425 nm, (2) 480 nm (3) 550 nm]. Overlapped decay curves of 3,2-HNA in PVA at concentration (e) 0.05 wt % and (f) 0.5 wt %.

Table 3, (Figure 3f), which shows the possibility of excimer formation. Thus, at higher concentration, a competition between ESIPT and excimer formation takes place in 3,2-HNA doped PVA film. Similar results were observed by Tarakka et al.<sup>7</sup> in the intramolecular hydrogen bonded polymer containing 2-hydroxyl phenyl benzoxazole and its derivative moiety in the main chain. These were used to explore the polymer structure extended conjugation and competition with excimer formation on ESIPT processes. Again the amplitude of 5.0 ns decay decreases on increasing concentration, indicating decrease in the percentage of monoanion. Unlike salicylic acid<sup>11</sup> in protic polymer (PVA), the dissociation of 3,2-HNA in PVA is not complete. At low concentration emission from rotamer R, rotamer P and monoanion is observed. Both inter and intramolecular proton transfer

takes place in PVA. The increase in the magnitude of the large Stokes shift in protic polymer, as compared with aprotic polymer, indicates more stabilization of ESIPT. The structures of various emitting species of 3,2-HNA trapped in PVA will be similar to Scheme 2, however, the aprotic polymer site will be changed by protic polymer site.

**3.1.3. In Nafion.** When 3,2-HNA is doped through ethanol solution, it shows structured absorption with maxima at 376 and 360 nm, respectively, and corresponding weak emission at 420 nm (B) along with a red band at 580 nm as shown in Figure 4a. The Stokes shifts of these bands are  $\sim 3900 \text{ cm}^{-1}$  and  $\sim 10\,500 \text{ cm}^{-1}$ , respectively, as given in Table 1. Similar Red band of 3,2-HNA is observed in acidic ethanol solution due to the presence of excess proton in the system which enhances the ESIPT by formation of zwitterion. The excitation spectra of both B and red bands are the same. Similar to aprotic polymer, on drying the film, the red band disappears and a new emission at 520 nm is observed. When 3,2-HNA is doped through water in Nafion film, the absorption is red shifted ( $\lambda_{\text{max}} = 425 \text{ nm}$ ), as compared to doping through ethanol, and a single broad emission band ( $\lambda_{\text{max}} = 530 \text{ nm}$ ) is observed (Figure 4b). The excitation spectrum for both B and G bands do not coincide

The time domain measurements for dye doped Nafion films are given in Table 4. The B emission band shows triple exponential fit with average decay time of 14, 2.5, and 0.49 ns with relative amplitude of intensity 53%, 41%, and 6%, respectively, as shown in Figure 4c. The longer wavelength emission decay shows double exponential. Relative amplitude of longer lifetime decreases and shorter lifetime increases with increase in emission wavelength as shown in Table 4. Red band emission ( $\lambda = 580 \text{ nm}$ ) shows single-exponential decay having decay time 0.39 ns. The green emission is biexponential with decay times 9.0 ns and 2.5 ns, respectively. The amplitude of shorter lifetime component decreases toward longer wavelength as shown in Table 4. This can be explained by the fact that Nafion has  $\text{SO}_3\text{H}^+$  polar headgroup as well as nonpolar fluorocarbon backbone. The cation of 3,2 HNA can be present in the vicinity of  $\text{SO}_3\text{H}^+$ , whereas neutral monomer will be present in nonpolar backbone as shown in Scheme 4. Due to the presence of the sulfonate group, Nafion film is highly hydrophilic; therefore, in water, the film is highly swollen and rotamer P or R can be present as cationic species.

These results indicate that the wet film doped through ethanol shows presence of rotamers P and R, which shows normal emission as well as ESIPT emission (580 nm). Presence of excess proton facilitates the ESIPT in zwitterionic species of rotamer P. The decay times 9.0 and 0.49 ns correspond to rotamer R and P species, respectively. Upon drying the film, the spectral characteristic, such as red shift in the absorption (425 nm) and corresponding green emission (530 nm) having Stokes shifts  $\sim 4600 \text{ cm}^{-1}$  and decay time 2.5 ns, shows the presence of cationic species. These results resemble those with low pH solution phase results.<sup>21</sup> Further, the decay time of 0.39 ns of red emission band corresponds to the ESIPT emission of tautomer of rotamer P. Thus the behavior of 3,2 HNA in Nafion polymer film is similar to SA.<sup>22</sup> The structures of various

**TABLE 3: Decay Data of 3,2-HNA in Protic Polymers:  $\lambda_{\text{Ex}} = 350 \text{ nm}$**

P	(M)	Em	$\tau_1(\text{ns})$	$\tau_2(\text{ns})$	$\tau_3(\text{ns})$	$\alpha_1\%$	$\alpha_2\%$	$\alpha_3\%$	$\chi^2_3$	$\chi^2_2$
PVA	0.02 wt. %	420	$12.9 \pm 0.09$	$0.94 \pm 0.01$	$4.75 \pm 0.04$	56	5	39	1.078	1.283
	0.02 wt. %	460	$11.4 \pm 0.01$	$1.21 \pm 0.03$	$4.65 \pm 0.03$	18	16	67	1.036	1.117
	0.02 wt. %	500	$8.69 \pm 0.01$	$1.90 \pm 0.05$	$4.55 \pm 0.02$	15	8	77	1.117	1.274
	0.5 wt. %	420	$10.9 \pm 0.04$	$0.91 \pm 0.01$	$4.47 \pm 0.02$	0.049	0.24	0.162	0.940	1.682
	0.5 wt. %	460	$10.8 \pm 0.06$	$1.23 \pm 0.04$	$4.60 \pm 0.02$	0.042	−0.70	0.152	1.123	2.121
	0.5 wt. %	500	$9.35 \pm 0.01$	$2.09 \pm 0.01$	$2.91 \pm 0.01$	0.032	−0.30	0.377	0.941	2.045

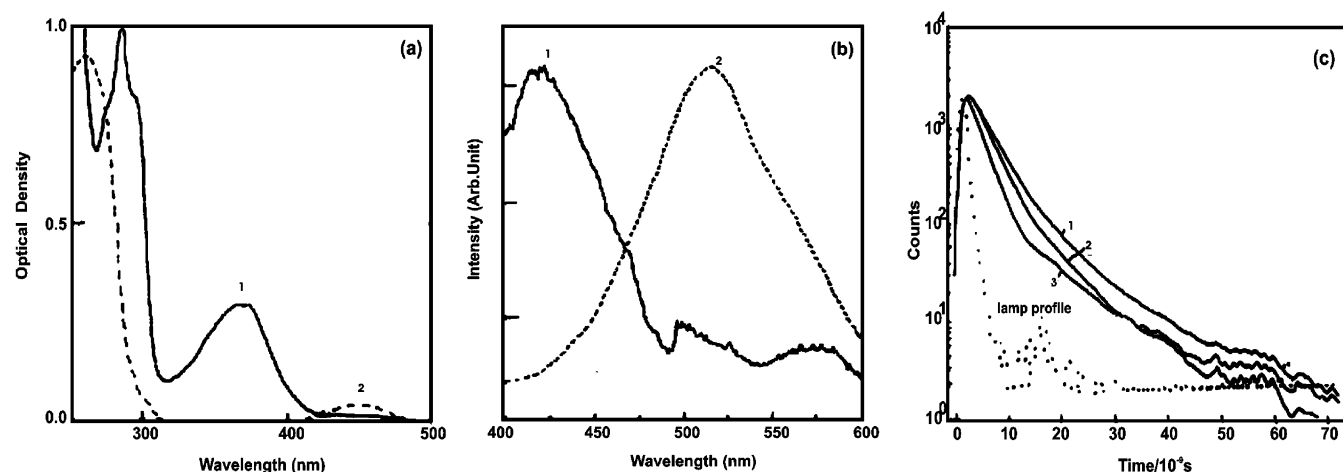
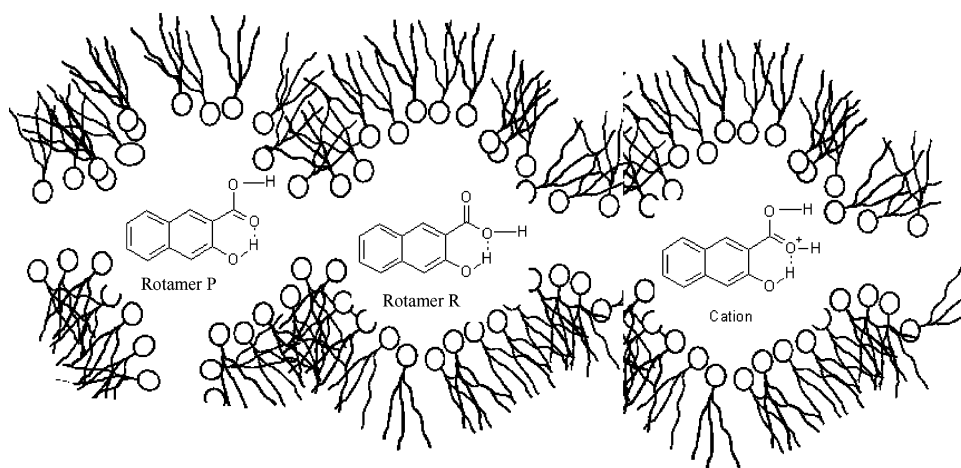


**Figure 4.** (a) Absorption spectra. (b) Normalized emission spectra ( $\lambda_{\text{ex}} = 360$  nm) of 3,2-HNA in Nafion film doped by (1) ethanol and (2) water. (c) Decay curves of 3,2-HNA in Nafion doped by ethanol [decay curve monitored ( $\lambda_{\text{em}}$ ) at (1) 460 nm, (2) 500 nm, (3) 560 nm with wavelength of excitation  $\lambda_{\text{ex}} = 360$  nm].

**TABLE 4: Decay Data of 3,2-HNA in Nafion Polymers:  $\lambda_{\text{ex}} = 350$  nm**

P	(M)	Em	$\tau_1$ (ns)	$\tau_2$ (ns)	$\tau_3$ (ns)	$\alpha_1\%$	$\alpha_2\%$	$\alpha_3\%$	$\chi^2_1$	$\chi^2_2$
Nafion	$\sim 10^{-5}$ M	420	$12.9 \pm 0.09$	$0.49 \pm 0.01$	$2.53 \pm 0.04$	56	5		1.065	1.332
		460	$9.78 \pm 0.01$		$2.79 \pm 0.03$	17		83	1.114	1.215
		500	$8.69 \pm 0.02$		$3.07 \pm 0.02$	20		80	1.071	2.581
		540	$9.73 \pm 0.05$		$3.06 \pm 0.08$	24		76	1.014	2.840

**SCHEME 4: Structures of Various Emitting Species of 3,2-HNA Trapped in Morphological Structure of Nafion Film**



emitting species of 3,2-HNA trapped in morphological structure of Nafion film are shown in Scheme 4.

**3.2. 1-Hydroxy-2-Naphthoic Acid (1,2-HNA).** The steady state and time domain parameters of 1,2-HNA in various polymers are given in Table 5.

**3.2.1. In Aprotic Polymers.** The absorption and emission spectra of 1,2-HNA in PMMA (L), PMMA (H), and CA are shown in Figure 5a. It shows three absorption bands at 245 nm, 280 nm ( $L_a$ ), and 350 nm ( $L_b$ ), respectively. The optical density of  $L_a$  and  $L_b$  band decreases as PMMA (L), PMMA (H) to CA. The emission corresponding to these bands shows both normal fluorescence 400 nm (blue emission) as well as phosphorescence in the range of 425–550 nm (green emission) as shown in Figure 5b. Slight shift in blue emission band is observed in these polymers. This may be due to change in microenvironment of the polymer matrix. Decay time measurements of fluorescence band show that the decay is biexponential having average decay time 3.5 ns (95%) and 6.3 ns (5%). The amplitude of the longer decay time slightly increases with increase in emission wave-

**TABLE 5: Photophysical Parameters of 1,2-HNA in Different Polymers<sup>a</sup>**

polymer	$\lambda_{\text{ab}}$ (nm)	$\lambda_{\text{em}}$ (nm)	stokes shift { $\nu_{\text{exc}} - \nu_{\text{em}}$ (max)} ( $\text{cm}^{-1}$ )	mean decay time ( $\tau$ ) (ns)	emitting species
PMMA (L)	350	405 (f) 425–550 (p)	3900	3.3, 6.4	rotamer P monoanion
PMMA (H)	350	400 (f) 425–550 (p)	3600	3.3, 6.4	rotamer P monoanion
CA	348	420 (f) 430–550 (p)	4200	3.4, 6.3	rotamer P monoanion
PVA	343	417 (f) 430–550 (p)	4500	3.6, 6.6	rotamer P monoanion
Nafion	365	452 (f)	5300	3.5, 1.9	rotamer P monocation

<sup>a</sup> (f) Indicate fluorescence and (p) indicate phosphorescence (decay time 2.5 s).

length, indicating the presence of two emitting species corresponding to a hydrogen bonded rotamer P and monoanion, respectively, similar to the solution phase results.<sup>23</sup> The percentage of monoanion is very small, therefore, no fluorescence

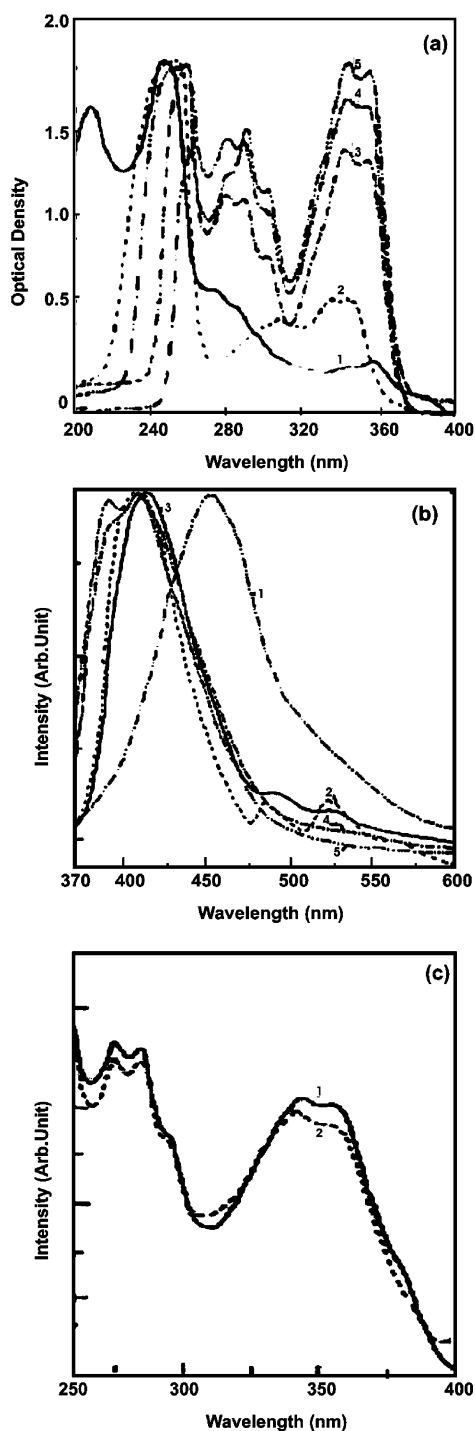
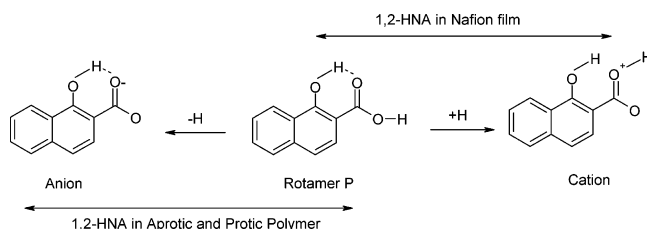


**Figure 5.** (a) Absorption spectra. (b) Normalized emission spectra of 1,2-HNA in (1) Nafion, (2) PVA, (3) CA, (4) PMMA (L) and (5) PMMA (H) polymer film. (c) Normalized excitation spectra of 1,2-HNA in PVA, emission monitored at (1)  $\lambda_{em} = 430$  nm and (2)  $\lambda_{em} = 525$  nm, respectively.

emission is observed. Further, the absence of longer decay time of blue emission indicates the absence of rotamer R of 1,2-HNA in these polymers. A slow decay ( $\sim 2.5$  s) due to phosphorescence emission similar to the halogen derivatives of the naphthalene is observed.<sup>40</sup>

**3.2.2. In Protic Polymer.** 1,2-HNA doped in PVA shows three absorption bands at 245 nm, 310 nm ( $L_a$ ), and 340 nm ( $L_b$ ) and corresponding fluorescence emission at 410 nm as well as phosphorescence in the range of 425–550 nm (Figure 5a,b). The  $L_a$  band is red shifted and  $L_b$  band is blue shifted in protic polymer as compared to aprotic polymers. The intensity of

#### SCHEME 5: Various Emitting Species of 1,2-HNA in Different Polymers



phosphorescence bands in PVA is higher than in aprotic polymers. Further the phosphorescence bands in PVA are highly humidity dependent and disappear on absorbing moisture by the film. The excitation spectra of both fluorescence and phosphorescence emissions coincides as shown in Figure 5c. Similar to aprotic polymers, the fluorescence decay in protic polymer fits to a biexponential function with average decay time 3.55 ns (92%) and 6.6 ns (8%), indicating the presence of two emitting species corresponding to hydrogen bonded rotamer P and monoanion respectively as in solution phase.<sup>23</sup> The slow decay time ( $\sim 2.0$  s) of green emission and overlapping of excitation spectra of both green & blue emission, indicates the photoinduced excited-state intersystem crossing and green emission from triplet state.

**3.2.3. In Nafion.** In Nafion film, 1,2-HNA shows three absorption bands at 240 nm, 260 nm ( $L_a$ ), and 368 nm ( $L_b$ ). The  $L_a$  band is blue shifted while  $L_b$  band is red shifted in Nafion film, as compared to aprotic and protic polymers. The fluorescence spectrum shows a band at 425 nm with Stokes shift of  $5273\text{ cm}^{-1}$ . No phosphorescence is detected in this film; this indicates the absence of intersystem crossing in 1,2-HNA species trapped in Nafion film. The increase of Stokes shift in Nafion film with respect to aprotic and protic polymers indicates the ESIPT is being more facile due to presence of an extra proton in very low pH environment of the polymer matrix. Further the dual decay time of 3.5 ns (20%) and 1.9 ns (80%) of 1,2-HNA in Nafion film corresponds to emission of neutral rotamer P and cationic species similar to as in solution phase.<sup>23</sup>

The various emitting species of 1,2-HNA in these polymers are shown in Scheme 5.

**3.3. Comparison of the Photophysics of 3,2-HNA with 1,2-HNA in Polymers.** Although the experimental and the theoretical investigations<sup>21–23</sup> show that intramolecular hydrogen bonding exists in both of these molecules, the photophysics and the photochemistry of these molecules are entirely different. Brief comparisons of these two molecules are given below.

Unlike 3,2-HNA, no ESIPT is observed in any molecular species of 1,2-HNA; however, it shows phosphorescence in aprotic and protic polymers. The intensity of phosphorescence band is higher in protic polymer than in aprotic polymers. The decreasing order of intensity of phosphorescence follows dry PVA > CA > PMMA (H) > PMMA (L). In similar conditions, no phosphorescence is detected for 3,2-HNA. This indicates that, in naphthalene molecules, having cross-linking with the conjugated chain, the ESIPT emission is quenched by the triplet. Unlike the aprotic and protic polymers, only blue fluorescence at 450 nm and no phosphorescence is observed in Nafion film. Unlike 3,2-HNA, the absence of longer decay time in 1,2-HNA indicates that the rotamer R type of species is not present in these polymers. Thus, the formation of IMHB by the substitution of OH group at  $\alpha$  (1) and  $\beta$  (3) positions in  $\beta$  (2)-naphthoic acid alter the photophysics of these two molecules in the micro-environment of the polymer. The former gives triplet emission while ESIPT is present in the later molecule.



**3.4. Correlation of Fluorescence Characteristics with Microenvironment.** The difference in both fluorescence intensity and decay behavior of 3,2-HNA in different polymers can be attributed to the change in the solvent polarity as well as free volume. The Stokes shift of the emission bands is related to micro-environmental changes both in the ground as well as excited state of the emitter.

The observed changes in the decay times are attributed partially from the free volume available in the polymer in the solid matrixes and partially from the species present in the polymer. The free volume is known to affect the local relaxation in polymer matrixes. Additionally, local relaxation of individual fluorophore affects the fluorescence behavior. Thus the magnitude of the ESIPT and lifetime correlation corroborates our earlier conclusions regarding the multicomponent decay due to various trapped geometries of the molecule. It can be seen that average decay time ( $\tau_{av}$ ) of the emitting species of 3,2-HNA changes across the emission profile, and it increases in order of Nafion < PVA < PMMA (L) < PMMA (H) < CA. As the solvent motion is almost frozen in the polymer, the observed decay behavior can be rationalized by assuming the trapping of the solute molecules in different geometry as different species. The relatively large change in  $\tau_{av}$  across the emission profile in case of Nafion and PVA can be partially attributed to more free volume available for the intramolecular motion of the solute, although there are more than one species of the molecules present in these polymers. However, in PMMA and CA, because of less free volume, the internal motion is restricted resulting in a very small change in  $\tau_{av}$ . Similar effects of polymer micro-environment on the photophysics of randomly distributed fluorophore have been observed in the literature.<sup>41,42</sup>

Further the observed change in fluorescence intensity of G band can be explained on the basis of the micro polarity of the matrix. As the micro polarity of the different polymer film increases, formation of monoanion increases and, hence, fluorescence intensity of the G band increases in the order PMMA (L) < PMMA (H) < CA < PVA. Earlier, Il'ichev et al.<sup>43</sup> also observed a similar effect of polarity, on intermolecular ESPT reactions in some long-chain derivatives of naphthols in solutions and Langmuir–Blodgett (LB) films. They found presence of ESIPT in 2-stearoyl-1-naphthol system in LB films and the absence of intermolecular ESPT between alkyl naphthols and the anion of stearic acid in LB films due to very low polarity of the interior of this film. Similarly, disappearance of phosphorescence emission by absorbing water indicates increase of nonradiative transition. Similar effect of change in the fluorescence characteristics of quinine sulfate dication doped (QSD) in different polymers<sup>42,44</sup> and sol–gel glasses<sup>45</sup> filled with solvent have been reported in the literature.

#### 4. Conclusions

These results suggest that both the molecules 3,2-HNA and 1,2-HNA are trapped as different emitting species in the different polymeric media, and their fluorescence characteristics are sensitive to micro-environmental polarity as well as free volume of the polymer matrix. Hydrogen bonded rotamer R, rotamer P, and mono anionic species of 3,2 HNA exist in aprotic and protic polymers. Rigidity of polymers decreases nonradiative transition and increases monoanion formation by an increase of dye to host polymer interaction due to increasing intermolecular hydrogen bonding with the binding site of the aprotic and protic polymer. This facilitates ESIPT in monoanionic form due to a strong intramolecular hydrogen bond. A competition between ESIPT and excimer formation is observed by the

appearance of rise time on increasing the concentration of 3,2-HNA in PVA polymer. In Nafion, both the molecules are present as a cationic as well as neutral species but ESIPT is observed only in 3,2-HNA monomer. In case of 1,2 HNA, ESIPT is not observed in any species trapped in these polymers; however, a very weak triplet emission (phosphorescence) is observed in aprotic and protic polymers. Further the absence of a longer decay time component in the blue emission indicates the nonexistence of rotamer R of 1,2 HNA in these polymers.

Presence of red emission band only in the solution phase of aprotic polymer of rotamer P of 3,2-HNA and the further appearance of higher intensity ratio of green emission in rigid polymer indicates dissociation of the doped molecule (3,2-HNA) is more in protic polymer with respect to aprotic polymer. This shows that interaction between the doped molecules to host polymer is weak in aprotic polymers while strong in protic polymer. Further, dissociation of 1,2-HNA is very weak with respect to 2,3-HNA in these polymers. It is observed that, depending on the position of the intramolecular hydrogen bond (IMHB) ring (whether linked at 1–2 or 3–2 position in the naphthalene system), the electronic spectra become modified. The micro-environment of the polymer affects the strength of IMHB and alters the photophysics of these intramolecular hydrogen-bonded molecules. Therefore, it is found that both photophysics and photochemistry of 3,2-HNA is different from that of 1,2-HNA.

**Acknowledgment.** Author is thankful to Prof. H. B. Tripathi and Dr. H. C. Joshi for valuable discussions and Dr. S. Pant for critical reading of the manuscript. Author is specially thankful to anonymous referee for valuable comments. Financial assistance in the form of Research Associate fellowship no. 9/428 (54) 2004, EMR-I from CSIR New Delhi, India is gratefully acknowledged.

#### References and Notes

- (1) Mishra, G. S. *Introductory Polymer Chemistry*; John Wiley and Sons: New York, 1993.
- (2) Barashkov, N. N.; Gunder, O. A. *Fluorescent Polymers*; Ellis Harwood: New York, 1994.
- (3) Hoyle, C. E.; Torkelson J. M. *Photophysics of Polymers*; ACS Symposium series 358; American Chemical Society: Washington, DC, 1987.
- (4) Demchenko, A. P. *Luminescence* **2002**, 17, 19.
- (5) Al-Hassan, K. A. *J. Polymer. Sci. B* **1988**, 26, 1727.
- (6) Birch, D. J. S.; Dutch, A.; Imof, R. E.; Davision, K. D.; Souton, I. *J. Polymer. Sci. B* **1987**, 27, 1273.
- (7) Tarakka, R. M.; Janekhe, S. A. *Chem. Phys. Lett.* **1996**, 260, 533.
- (8) Gunter, P.; Huignard, J. P. In *Photorefractive Materials and their Applications*; Springer-Verlag: Berlin, 1989; Vols. 2.
- (9) Costela, A.; Sastre, R. *Appl. Phys. B* **1995**, 60, 383.
- (10) Acuna, U.; Gueni, F. A.; Costela, A.; Dauhal, A.; Figurea, J. M.; Florido, F.; Sastre, R. *Chem. Phys. Lett.* **1991**, 187, 98.
- (11) Mishra, H.; Misra, V.; Mehata, M. S.; Pant, T. C.; Tripathi, H. B. *J. Phys. Chem. A* **2004**, 108, 2346.
- (12) Misra, V.; Mishra, H.; Joshi, H. C.; Pant, T. C. *Sensors and Actuators* **2002**, 82, 133.
- (13) Geddes, G. D. *Meas. Sci. Technol.* **2001**, 12, 53.
- (14) Vollmer, F.; Rettig, W. *J. Photochem. Photobiol., A: Chem.* **1996**, 95, 143.
- (15) Douhal, A.; Dabrio, J.; Sastre, R. *J. Phys. Chem. A* **1996**, 100, 149.
- (16) Kalyansundaram, K. *Photochemistry in Micro Heterogeneous System*; Academic Press: New York, 1989.
- (17) Das, S. K.; Dogra, S. K. *J. Colloid Interface Sci.* **1998**, 205, 443.
- (18) Ramamurthy, V. *Photochemistry in Organized and Constrained Media*; VCH Publishers: New York, 1991.
- (19) Brotulos, P.; Monti, S. *Adv. Photochem.* **1995**, 21, 1.
- (20) Borgis, D. In *Electron and Proton Transfer in Chemistry and Biology*; Muller, A., Ratajczk, D. W., Eds.; Elsevier: Amstertam, 1992.

- (21) Mishra, H.; Joshi, H. C.; Tripathi, H. B.; Maheshwary, S.; Sathyamurthy, N.; Panda, M.; Chandrasekhar, J. *J. Photochem. Photobiol., A: Chem.* **2001**, *139*, 23.
- (22) Mishra, H. Photoinduced Electronic Eexcited-State Relaxation and Proton-Transfer Phenomena in some Hydrogen Bonded Molecular Systems, Ph.D. Thesis, Kumaun University India, 2002.
- (23) Mishra, H.; Maheshwary, S.; Tripathi, H. B.; Sathyamurthy, N. *J. Phys. Chem. A* **2005**, *109*, 2746.
- (24) Mishra, H. *Chem. Phys Lett.* 2005, (to be communicated).
- (25) Golubev, N. S.; Denisov, G. S.; Kuzina, L. A.; Smirnov, S. N. *J. General Chem. (Russ)* **1994**, *64*, 1162.
- (26) Schulman, S. G.; Kovi, P. J. *Anal. Chim. Acta* **1973**, *67*, 267.
- (27) Tolbert, L. M.; Solntsev, K. M. *J. Acc. Chem. Res.* **2002**, *35*, 19.
- (28) Woolfe, G. J.; Thistlethwaite, P. J. *J. Am. Chem. Soc.* **1981**, *103*, 3849.
- (29) Woolfe, G. J.; Thistlethwaite, P. J. *J. Am. Chem. Soc.* **1980**, *102*, 6917.
- (30) Law, K.-Y.; Shoham, J. *J. Phys. Chem.* **1994**, *98*, 3114.
- (31) Kovi, P. J.; Shulman, S. G. *Anal. Chem.* **1973**, *45*, 989.
- (32) Kovi, P. J.; Miller, C. L.; Schulman, S. G. *Anal. Chim. Acta* **1972**, *61*, 7.
- (33) Klessinger M.; Michel J. *Excited State and Photochemistry of Organic Molecules*; VCH Publishers: New York, 1995; p 47.
- (34) Catalán, J.; del Valle, J. C.; Palomar, J.; Diaz, C.; de Paz, J. L. G. *J. Phys. Chem. A* **1999**, *103*, 10921.
- (35) Banerjee, D.; Mandal, A.; Mukherjee, S. *Chem. Phys. Lett.* **2002**, *357*, 450.
- (36) Chowdhury, P.; Chakravorti, S. *Chem. Phys. Lett.* **2004**, *395*, 103.
- (37) Mishra, H.; Tripathi, H. B.; Pant, D. D. *Rev. Sci. Inst.* (in press).
- (38) Fujji, T.; Yamamoto, H.; Takanaka, H.; Yobilo, Y.; Anpo, M. *J. Chem. Soc., Faraday Trans* **1995**, *91*, 4279.
- (39) Joshi, H. C.; Mishra, H.; Tripathi, H. B. *J. Photochem. Photobiol., A: Chem.* **1997**, *105*, 15.
- (40) Turro, N. J. *Modern Molecular Photochemistry*; The Benjamin/Cummings Publishing Co. Inc.: San Francisco, 1978; p 115.
- (41) Bright, V.; Munson, C. A. *Anal. Chim. Acta* **2003**, *500*, 71.
- (42) Joshi, H. C.; Upadhyay, A.; Mishra, H.; Tripathi, H. B.; Pant, D. D. *J. Photochem. Photobiol., A: Chem.* **1999**, *122*, 185.
- (43) Il'ichev, Y. V.; Solntsev, K. M.; Demyashkevich, A. B.; Kuzmin, M. G.; Lemmetyinen, H.; Vuorimaa, E. *Chem. Phys. Lett.* **1992**, *193*, 128.
- (44) Nava, M. A.; Garcia, M. O. B.; Torres, L. A. D.; Cenda, S. C.; Kong T. A. *Opt. Mater.* **1999**, *13*, 327.
- (45) Rocha, C. J.; Gehlen, M. H.; Silva, R D.; Donate, P. M. *J. Photochem. Photobiol., A Chem.* **1999**, *123*, 129.